WPSA-CPR(18) 19895

D Corona et al.

Plasma shape control assessment for JT-60SA using the CREATE tools

Preprint of Paper to be submitted for publication in Proceeding of
30th Symposium on Fusion Technology (SOFT)

This work has been carried out within the framework of the EUROfusion Consortium and has received funding from the Euratom research and training programme 2014-2018 under grant agreement No 633053. The views and opinions expressed herein do not necessarily reflect those of the European Commission.

Plasma shape control assessment for JT-60SA using the CREATE tools

D. Corona[a], N. Cruz[a], G. De Tommasi[b,c], H. Fernandes[a], E. Joffrin[d], M. Mattei[e,c], A. Mele[b,c], Y. Miyata[f], A. Pironti[b,c], T. Suzuki[f], H. Urano[f], F. Villone[b,c]

[a] *Instituto de Plasmas e Fusão Nuclear, Instituto Superior Técnico, Universidade de Lisboa, 1049-001 Lisboa, Portugal*
[b] *Dipartimento di Ingegneria Elettrica e delle Tecnologie dell'Informazione, Università degli Studi di Napoli Federico II, via Claudio 21, 80125, Napoli, Italy*
[c] *Consorzio CREATE, via Claudio 21, 80125, Napoli, Italy*
[d] *CEA, IRFM, F-13108 Saint-Paul-lez-Durance, France*
[e] *Dipartimento di Ingegneria, Università degli Studi della Campania Luigi Vanvitelli, via Roma 29, Aversa (CE), 80131, Italy*
[f] *National Institutes for Quantum and Radiological Science and Technology, Naka, Ibaraki, 311-0193, Japan*

Abstract

This paper proposes a plasma shape controller for JT-60SA based on the *eXtreme Shape Controller* approach originally implemented for the JET tokamak. The controller is designed using the CREATE linear model for the plasma-circuit response. JT-60SA represents a relevant benchmark to further validate this control approach given the high beta regimes that are envisaged during its operation. Indeed, such regimes represent a challenge from the plasma magnetic control perspective.

The performance of the proposed controller has been assessed with the aim of defining an *optimal* set of gaps to be controlled. The capability of tracking different plasma shapes, as well as the one of rejecting disturbances has been considered. The result of this analysis suggests that a set of about 20 gaps equally spaced along the plasma boundary permits to control the shape with a steady-state root-mean square error of less than 1 cm during the flattop of JT-60SA Scenario 2, for the considered test cases.

Keywords: JT-60SA, plasma magnetic control in tokamak, plasma shape control, benchmarking

1. Introduction

The Satellite Tokamak Programme (STP) is the main project within the Broader Approach agreement. The STP includes the construction of the JT-60SA superconductive tokamak and its exploitation as an ITER "satellite" facility [1]. In view of JT-60SA operations, Japanese and European scientists are developing different tools to support preliminary studies. In this context, a set of modelling tools for the design and the validation of plasma magnetic control have been developed [2].

Plasma magnetic control is needed since early tokamak operations to drive the currents in the external active coils, in order to achieve plasma breakdown and to track the scenario current waveforms. In [3], the CREATE electromagnetic modelling tools were used to design and validate a set of control algorithms for JT-60SA. An *isoflux* approach was proposed for plasma shape control, similarly to what has been done in [4, 5] and [6]. In particular, the control design procedure used in [3] is based on the *eXtreme Shape Controller* (XSC) approach, which has been adopted at JET since 2003 [7], and has been recently used to obtain high triangularity shapes with both strike points in the divertor corner, which has a large impact in the H-mode confinement in the case of ITER-like wall at JET [8].

In this work, the XSC approach is used to design a *gap-based* plasma shape controller for JT-60SA[1]. Indeed, JT-60SA represents a relevant benchmark to further validate the *gap-based* control approach, given the high beta regimes that are envisaged during its operation, which represent a challenge from the plasma magnetic control perspective.

Different test cases are considered to assess the performance of the proposed shape controller, with the aim of defining an *optimal* set of gaps to be controlled. In particular, the capability of tracking different plasma shapes, as well as the one of rejecting the envisaged disturbances is considered.

The rest of this paper is organized as follows. Section 2 briefly introduces the XSC control strategy, while the reference scenario considered to assess the performance of the gap-based controller is introduced in Section 3, as well as the various disturbances used to run the simulations. The main contribution of this paper is then given in Section 4, where the results of the simulations that have been carried out to assess the controller performance are presented. Some conclusive remarks are eventually given.

2. Gap-based algorithm for plasma shape control at JT-60SA

In this section the XSC control algorithm is briefly recalled. This algorithm is used in Section 4 to evaluate the steady-state performance of the plasma shape controller under different choices for *gaps* to be controlled. It is

Email address: `lilia.rivera@tecnico.ulisboa.pt` (D. Corona)

[1]It should be noticed that the *isoflux* strategy is the only viable solution for plasma boundary control at a beginning of a plasma discharge. Indeed, at relatively low values of plasma current, the noise on the magnetic measurements usually causes a relatively big error on real-time plasma boundary reconstruction. For this reason at the beginning of the discharge, isoflux control is usually adopted. However, gap-based control may enhance the flexibility of the plasma shape controller at the flattop.

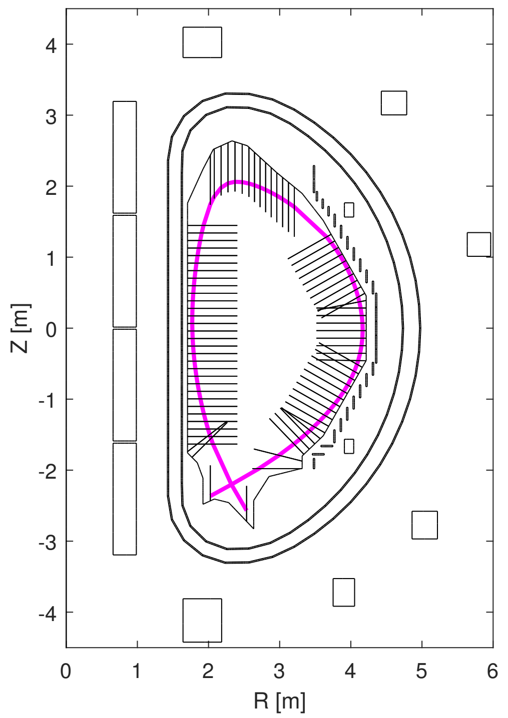

Figure 1: Poloidal cross-section of the JT-60SA plasma at the Start of the Flat Top (SOF) for reference Scenario 2. At SOF, the nominal plasma current is 5.5 MA, while the nominal values for poloidal beta β_p and internal inductance l_i are 0.53 and 0.85, respectively. In this figure the 85 gaps used to assess the plasma shape controller performance are shown.

worth to remark that the XSC is just one of the possible control strategies, and that it can be adopted both for gap-based (as in JET [9]) or for isoflux plasma shape control (as at EAST [10]). The peculiarity of the XSC approach is that it permits to control a number of plasma shape descriptors that is greater than the number of available actuators, i.e. of Poloidal Field Circuits (PFC). More details about the XSC algorithm can be found in [11].

Fig. 3(a) shows a poloidal cross-section of JT-60SA together with the gaps used in this paper for the assessment of the plasma shape control. The gaps are segments that can be used to describe the shape of the plasma boundary.

Being g_i the abscissa along the i-th control segment, we assume that $g_i = 0$ at the first wall. *Gap-based* plasma shape control is achieved by controlling to zero the difference $g_{i_{ref}} - g_i$ on a sufficiently large number of gaps, being g_{i_ref} the value of the abscissa on the i-th control segment for the reference shape.

The XSC algorithm can be used either to implement a *gap-based* control strategy, or an *isoflux* one, as it has been proposed in [3]. The peculiarity of XSC is that it permits to track a number of shape parameters larger than the number of PFC. This goal is achieved by minimizing a weighted steady-state quadratic tracking error, when the references are constant signals, rather than control it to zero.

The XSC control relies on the PFC decoupling controller (more details can be found in [3, Section 4.4]), since it is assumed that each PFC can be treated as an independent single-input-single-output channel whose dynamic response is modeled in the Laplace domain by

$$I_{PF_i}(s) = \frac{I_{PF_{ref,i}}(s)}{1 + s\tau_{PF}},$$

where I_{PF_i} and $I_{PF_{ref_i}}$ are the Laplace transform of the measured and reference current in the i-th PFC, respectively, and where it is assumed that all the PFC exhibit the same bandwidth (i.e., they have the same time constant τ_{PF}).

Denoting by $\delta Y(s)$ the Laplace transform of the variations of the n_G gaps to be controlled, it is possible to exploit the CREATE electromagnetic linear model [3] that links the variation of the PFC reference currents $\delta I_{PF_{ref}}$ to $\delta Y(s)$, i.e.

$$\delta Y(s) = C \frac{\delta I_{PF_{ref}}(s)}{1 + s\tau_{PF}},$$

which, at steady-state, implies $\delta Y(s) = C \delta I_{PF_{ref}}(s)$.

If the number of controlled plasma shape descriptors n_G is such that $n_G > n_{PF}$, the XSC computes the additional current references as

$$\delta I_{PF_{ref}} = C^{\dagger} \delta Y . \qquad (1)$$

where the matrix $C^{\dagger}$ denotes the pseudo-inverse of C that can be computed via the singular value decomposition (SVD). As a result, the XSC algorithm minimizes the following steady-state performance index

$$J_{XSC} = \lim_{t \to +\infty} (\delta Y_{ref} - \delta Y(t))^T (\delta Y_{ref} - \delta Y(t)), \qquad (2)$$

where δY_{ref} are constant references for the geometrical descriptors. When the SVD of the C matrix is used to minimize (2), it may happen that some singular values (depending on the plasma configuration) are one order of magnitude smaller than the others. This fact implies that minimizing the performance index (2) retaining all the singular values results in a large control effort at the steady-state, that is a large request on some PFC currents which have only a minor effect on the plasma shape. In order to minimize also the control effort, the additional references (1) are generated by using only the $\bar{n} < n_{PF}$ linear combinations of PF currents which are related to the largest singular values of the C matrix. This is achieved by using only the $\bar{n}$ singular values when computing the pseudo-inverse $C^{\dagger}$.

Moreover, the PFC current variations given by (1) are summed to the scenario currents and sent to the PFC decoupling controller as references to be tracked. It is worth to remark here that the dynamnic behaviour of the XSC is improved by adding a set of proportional-integral-derivative (PID) controllers on each PFC channel (see [11] for a complete description of the XSC control scheme).

3. Reference scenario for the performance assessment

This section introduces the reference scenario considered in this paper. Furthermore, the test cases used in Section 4 to assess the performance of the considered shape controller by means of simulations, are also presented. These test cases include a set of envisaged disturbances to be rejected, which have been taken from [6] and [12].

The considered scenario is the so-called *Scenario 2* which is one of the references used for the design of JT-60SA [12, Sec. 1.2].

In particular, Scenario 2 refers to a 5.5 MA inductive lower single null discharge, whose reference shape at *Start of Flattop* (SOF) is shown in Fig. 3(a). Given the magnetic equilibrium at SOF, using the CREATE codes [13, 14] it is possible to retrieve a linearized model that describes the plasma magnetic behaviour around that equilibrium[2]. The nominal values for the plasma current, the poloidal beta and the internal inductance for Scenario 2 at SOF are $I_{p_{eq}} = 5.5$ MA, $\beta_{p_{eq}} = 0.53$, and $l_{i_{eq}} = 0.85$.

The linearized model of Scenario 2 at SOF has been used to design the proposed gap-based shape controller, as well as to assess its performance via simulations. In order to perform the latter task, the following set of disturbances have been considered. It should be noticed that, as far as plasma magnetic control is concerned, the disturbances have been modeled has variations of β_p and l_i.

- **Disturbance #1** refers to the behaviour of β_p and l_i soon after the current flattop is reached, as it was modeled in [6] (in this paper we assume that the flattop is reached at $t \sim 16$ s). As an example, the correspondent time traces are shown in Fig. 2[3].
- **Disturbance #2** refers to the behaviour of β_p due to the presence of an Edge-Localized Mode (ELM). As described in [12, p. 34], during the flattop an instantaneous drop in β_p of $0.05\ \beta_{p_{eq}}$ is followed by and exponential recovery with a time constant of 0.05 s with a frequency 10 Hz. Note that for this disturbance l_i does not change.
- **Disturbance #3** describes an instantaneous drop in l_i of 0.2 $(l_{i_{eq}} - 0.5)$ without recovery, simultaneous with a drop on β_p of 0.2 $\beta_{p_{eq}}$ followed by a recovery exponential time of 1 s [12, p. 34], which are typical of a so called *minor disruption*.

4. Performance assessment

In this section we summarize the results of the analysis aimed at assessing an set of gaps to be controlled, which represents a good trade-off between performance of the shape control and number of controlled variables.

In order to perform the above mentioned assessment, all around the first wall an equally spaced distribution of 85 gaps was considered as shown in Fig. 3(a). It should be noticed that all different selections of controlled gaps considered in this paper include the two vertical gaps in the divertor zone, which allows to control the strike-points, and hence the position of the X-point.

Other than the whole set of 85 gaps shown in Fig. 3(a), in this paper three additional choices are considered. The first one is reported in Fig. 3(b), which consists of 20 gaps equally spaced along the first wall. Moreover, the selection of 8 and 6 gaps that correspond with the control segments considered by the isoflux controllers presented in [4] and [5], respectively, have been also considered (see Figs. 3(c) and 3(d)).

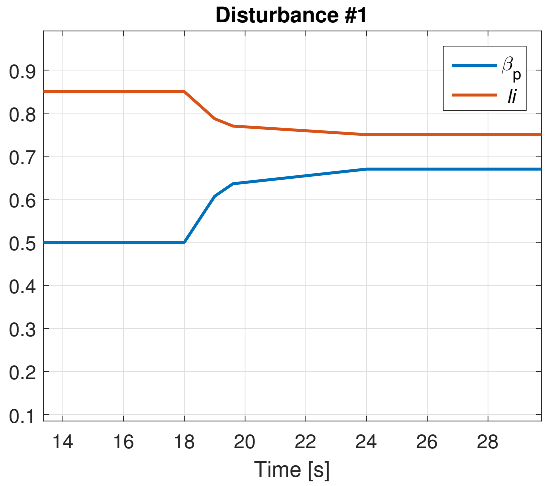

Figure 2: Poloidal beta and internal inductance time traces for Disturbance #1 that models the expected disturbance soon after the plasma current flattop is reached (at $t \sim 16$ s), according to what has been considered in [6].

The comparison between the various considered gap sets for the considered test cases is summarized in Table 1. This table shows the *root-mean-square error* (RMSE) between the reference shape and the shape obtained at steady-state after the occurrence of the disturbances. For all the cases reported in Table 1, the RMSE has been computed on the set of 85 gaps shown in Fig. 3(a), even when not all of them are controlled.

It turns out that, according to this preliminary analysis, the rejection of the disturbances induced by ELMs is not an issues at JT-60SA, whatever is the set of gaps that is controlled.

On the other hand, for the other two considered cases, at steady-state, the selection of 85 and 20 gaps have a considerable better RMSE in comparison with the selection of 8 and 6 gaps. As outlined in Table 1, the worst case corresponds to the selection of 8 gaps with the presence of Disturbance #3 (minor disruption) during the flattop. As an example, Fig. 4 shows a comparison of the steady-state shape obtained for the 8 and 20 gaps options. Fig. 5 shows the RMSE time traces for the case for Disturbance #3, and it can be noticed that the 20 gaps option gives better results with respect to the 8 and 6 gaps cases also during the transient, and not just in steady-state.

Moreover, if we consider the two options with 85 and 20 equally spaced gaps, it can be noticed that there is no practical difference. For these two options, whatever test case is considered there is no practical difference between the reference shape and the one attained at steady-state. It follows that, within the considered configurations, the 20 gaps selection represents the *optimal* choice for the set of gaps to be controlled assuming a XSC-like control approach, since it guarantees RMSE along the overall plasma boundary at steady-state of less than 1 cm for the considered test cases.

[2]For more details about the use of the CREATE equilibrium codes to retrieve plasma linearized models, the interested reader can refer to [3, Sec. 3].

[3]The time behaviour of both β_p and l_i have been estimated starting from the spatial profiles for both plasma density and temperature envisaged for Scenario 2.

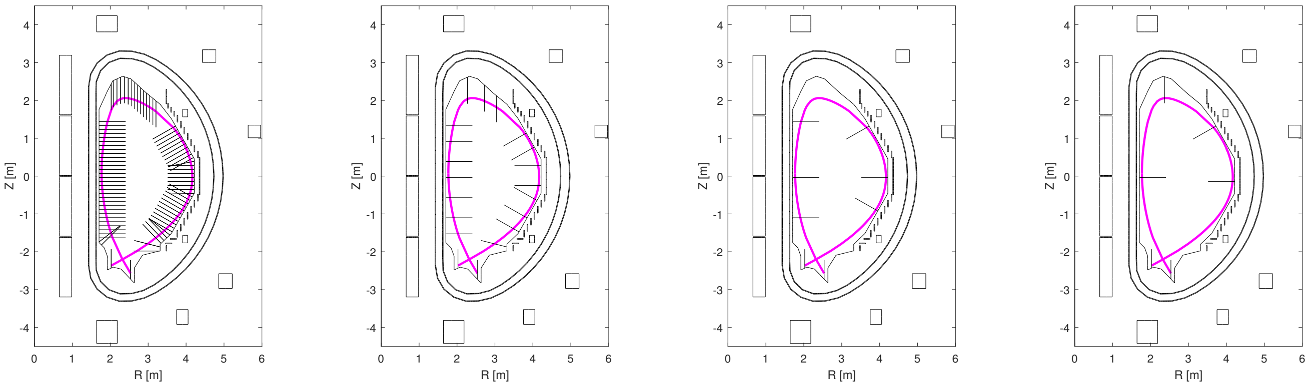

(a) The 85 gaps used to assess the performance of plasma shape controller in Section 4.

(b) The 20 gaps used to assess the performance of plasma shape controller in Section 4.

(c) The 8 control segments by the isoflux controller proposed in [4].

(d) The 6 control segments used by the isoflux controller proposed in [5].

Figure 3: Different choices for the set of controlled gaps used in Section 4.

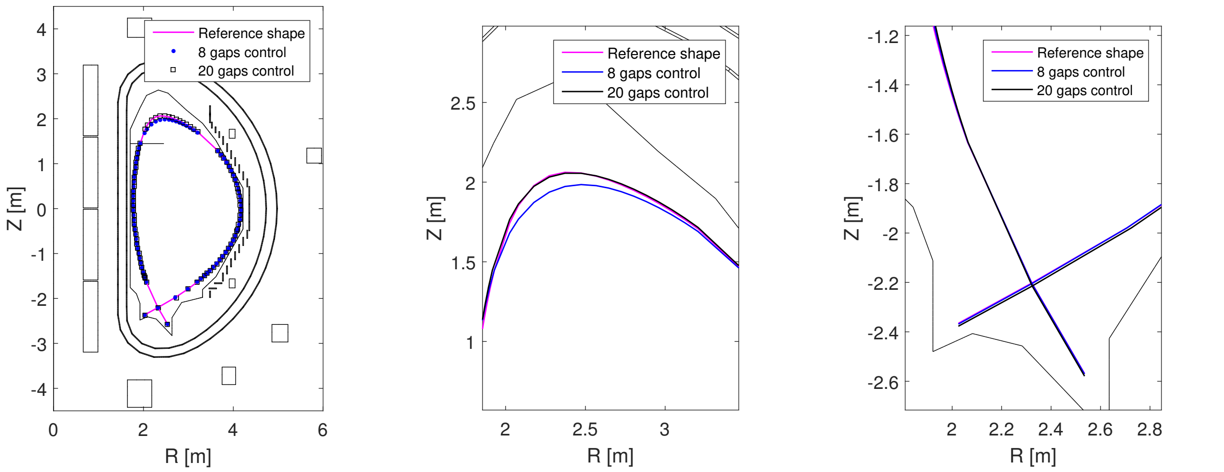

(a) Poloidal cross-section of JT-60SA.

(b) Detailed view of the top region.

(c) Detailed view of the divertor region.

Figure 4: Comparison of the shape controller performance in the presence of Disturbance #3 (minor disruption). The two cases of 8 and 20 gaps are considered.

Steady-state RMSE [mm]				
	85 Gaps	20 Gaps	8 Gaps	6 Gaps
Disturbance #1	7.7	8.7	31.2	19.8
Disturbance #2	~ 0	~ 0	~ 0	~ 0
Disturbance #3	6.1	7.8	26.9	16.3

Table 1: RMSE values for different choices of controlled gaps and for the different test cases that have been considered in Section 4. For all the reported cases the RMSE has been computed on the set of 85 gaps shown in Fig. 3(a).

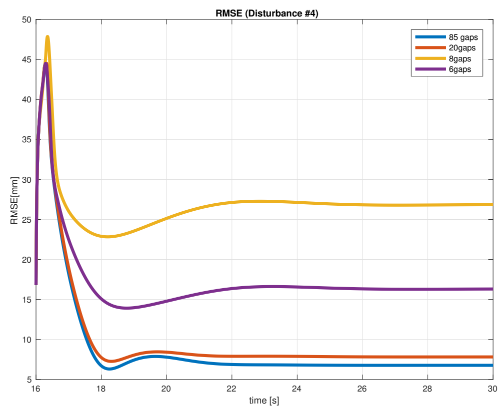

Figure 5: RMSE time traces for the different gaps selections when Disturbance #3 (minor disruption).

Conclusions

A comparison between different sets of controlled gaps has been carried out in this paper, assuming a XSC-like approach for the plasma shape control, and a linear plasma response for the JT-60SA Scenario 2 plasma. Different test cases have been considered to assess the control performance, which has been evaluated on the basis of the RMSE between the reference shape and the one obtained by the controller at steady-state. The results of this preliminary study suggest that a set of about 20 equally spaced gaps represent a good trade-off between steady-state performance and number of variables to be controlled, since it permits to control the shape with a steady-state RMSE of less than 1 cm for the considered test cases. Moreover, 20 controlled gaps is a result similar to the one used at JET, where the XSC controls about 30 gaps.

The presented results also indicate that the selection of 8 and 6 shape descriptors proposed in [4] and [5] reveals a greater RMSE value for the considered test cases. This is due to the few number of controlled gaps, especially in the top and inner side regions.

It should be remarked that, in order to further validate this preliminary results, the set of selected gaps needs to be tested also on JT-60SA relevant scenarios other than Scenario 2.

Acknowledgements

This work has been carried out within the framework of the EUROfusion Consortium and has received funding from the Euratom research and training programme 2014-2018 under grant agreement No 633053. The views and opinions expressed herein do not necessarily reflect those of the European Commission. The work of D. Corona was also funded by "Fundação para a Ciência e Tecnologia" (FCT) under grant No. **PD/BD/114306/2016** carried out as part of the training in the framework of the Advanced Program in Plasma Science and Engineering (APPLAuSE, sponsored by FCT under grant No. PD/00505/2012). "Instituto Superior Técnico" (IST) activities also received financial support from FCT through project UID/FIS/50010/2013. The views and opinions expressed herein do not necessarily reflect those of FCT, of IST or of their services.

References

[1] H. Shirai, et al., Recent progress of the JT-60SA project, Nucl. Fus. 57 (2017) 102002.

[2] G. Giruzzi, et al., Physics and operation oriented activities in preparation of the JT-60SA tokamak exploitation, Nucl. Fus. 57 (2017) 085001.

[3] N. Cruz, et al., Control-oriented tools for the design and validation of the JT-60SA magnetic control system, Contr. Eng. Prac. 63 (2017) 81–90.

[4] Y. Miyata, et al., Study of JT-60SA Operation Scenario using a Plasma Equilibrium Control Simulator, Plasma and Fus. Res. 8 (2013) 2405109–2405109.

[5] Y. Miyata, T. Suzuki, S. Ide, H. Urano, Study of Plasma Equilibrium Control for JT-60SA using MECS, Plasma and Fus. Res. 9 (2014) 3403045–5.

[6] H. Urano, et al., Development of operation scenarios for plasma breakdown and current ramp-up phases in JT-60SA tokamak, Fus. Eng. Des. 100 (2015) 345–356.

[7] G. Ambrosino, et al., Design and Implementation of an Output Regulation Controller for the JET Tokamak, IEEE Trans. Control Syst. Tech. 16 (2008) 1101–1111.

[8] E. de la Luna, et al., Recent Results on High-Triangularity H-Mode Studies in JET-ILW, in: 26th IAEA Fusion Energy Conference, Kyoto, Japan.

[9] G. De Tommasi, et al., Shape Control with the eXtreme Shape Controller During Plasma Current Ramp-Up and Ramp-Down at the JET Tokamak, J. Fus. Energy 33 (2014) 149–157.

[10] R. Albanese, et al., A MIMO architecture for integrated control of plasma shape and flux expansion for the EAST tokamak, in: Proc. of the 2016 IEEE Multi-Conf. Syst. Contr., Buenos Aires, Argentina, pp. 611–616.

[11] M. Ariola, A. Pironti, The design of the eXtreme Shape Controller for the JET tokamak, IEEE Control Sys. Mag. 25 (2005) 65–75.

[12] JT-60SA Team, Plant Integration Document, Technical Report, 2017. Https://users.jt60sa.org/?uid=222UJY.

[13] R. Albanese, R. Ambrosino, M. Mattei, CREATE-NL+: A robust control-oriented free boundary dynamic plasma equilibrium solver, Fus. Eng. Des. 96–97 (2015) 664–667.

[14] F. Villone, P. Vyas, J. Lister, R. Albanese, Comparison of the CREATE-L plasma response model with TCV limited discharges, Nucl. Fus. 37 (1997) 1395–1410.